QATAR UNIVERSITY

COLLEGE OF ENGINEERING

IM-BASED MULTIPLE ACCESS TECHNIQUES IN 5G NETWORKS: A NOVEL SCHEME AND PERFORMANCE ANALYSIS

BY

ABDULLATEEF ALMOHAMAD

A Thesis Submitted to

the College of Engineering

in Partial Fulfillment of the Requirements for the Degree of

Masters of Science in Electrical Engineering

June 2021

COMMITTEE PAGE

The members of the Committee approve the Thesis of
Abdullateef Almohamad defended on 11/04/2021.

Prof. Mazen O. Hasna
Thesis/Dissertation Supervisor

Prof. Saud Althunibat
Thesis/Dissertation Co-Supervisor

Prof. Tamer Khattab
Committee Member

Prof. Ali Ghrayeb
Committee Member

Approved:

Khalid Kamal Naji, Dean, College of Engineering

ABSTRACT

ALMOHAMAD, ABDULLATEEF., Masters: June: 2021,

Masters of Science in Electrical Engineering

Title: IM-Based Multiple Access Techniques in 5G Networks: A Novel Scheme and Performance Analysis

Supervisor of Thesis: Prof. Mazen O. Hasna.

Co-Supervisor of Thesis: Dr. Saud Althunibat.

In the next generations of communication systems, resources' scarcity devolves to a more critical point as a consequence of the expected massive number of users to be served. Furthermore, the users' contradicting requirements on quality of service forces the network to behave in a dynamic way in terms of the multiple access orchestration and resource assignment between users. Hence, the linear relation between the number of served users and the required (orthogonal or semi-orthogonal) resources is no longer sufficient as in the orthogonal multiple access (OMA) schemes.

Non-orthogonal multiple access (NOMA) schemes and index modulation (IM) techniques emerge as candidates to satisfy the ever-increasing spectral efficiency and connectivity demands. In this thesis, a comprehensive literature review is conducted on the IM-based multiple access techniques, and a novel IM-based NOMA downlink scheme, termed as IM-NOMA, is proposed, where the Base Station (BS) selects a channel or more to serve each user based on the IM concept and the corresponding power level is allocated based on the NOMA concept. At the users' ends, two detection techniques, namely maximum likelihood (ML) and successive interference cancellation (SIC), are considered and their error rate, outage probability and

computational complexity are analyzed. Furthermore, a low computationally complex detection technique is designed for the proposed IM-NOMA scheme. Multiple numerical simulations are conducted to verify the efficiency of the proposed scheme and to validate the analytical findings. Simulation results show the accuracy of the analytical formulas and that the proposed IM-NOMA can outperform the conventional NOMA scheme and the related state-of-the art schemes in terms of error performance.

DEDICATION

To my parents, brothers, and sisters

ACKNOWLEDGMENTS

I would like to express my sincere gratitude to my supervisors, Prof. Mazen Hasna and Dr. Saud Althunibat, for their patience, support, understanding and invaluable advices. I would like to extend my profonde appreciation to Prof. Hasna who believed in me, assisted me to keep on track and supported my very first steps into the research world. I am deeply grateful to the Qatar National Research Fund (QNRF) who has got me covered throughout my studies, this work would not come to existence without their support. Finally, my appreciation goes to my parents and my ten siblings for their unconditional love, support, and encouragement.

TABLE OF CONTENTS

LIST OF FIGURES

CHAPTER 1: INTRODUCTION

1.1 Background

While 5G communication technology is about to be standardized and launched, a set of challenging requirements are still pending to be met. In fact, next generation networks have to be more flexible and dynamic to meet the contradicting quality of service (QoS) requirements by different users being served by the same network. Thus, trade-off-based solutions are no longer sufficient in general. Moreover, an explosion in the number of connected users is expected in future wireless networks. Therefore, and taking into consideration the scarce spectrum and the limited energy resources, innovative systems and schemes have to be developed and standardized on the way to achieve the 5G targets [1].

The adopted multiple access (MA) scheme, in a communication system, plays the most prominent role in determining both spectral efficiency and connectivity capacity. Generally, MA orchestration is either done in an orthogonal (OMA) or a non-orthogonal (NOMA) fashion [2]. In OMA schemes, the time, frequency, or code resources are divided into orthogonal resource blocks (RB) and a single user is allocated to a single orthogonal RB as in (TDMA, FDMA or CDMA) schemes, respectively. On the other hand, NOMA schemes allow multiple users to share the available resources at the same time, which improves the spectral efficiency and connectivity [3]. In NOMA, users' signals can be spread in power domain (PD-NOMA) [4] or in code domain as in sparse code multiple access (SCMA) [5]. Thus, successive interference cancellation (SIC) techniques are applied at the receiver to cancel the introduced inter-user interference. In PD-NOMA, which is the most common scheme in the literature, different power levels are assigned to users based on their channel conditions, in which more power is allocated to the user with poor channel and vice versa. Therefore, fairness between users can be achieved by tuning

the power distribution coefficients among users [6]. NOMA has been widely investigated in the literature, and nominated as an efficient solution for the future systems. Index modulation (IM) [7] is another promising physical layer solution that aims at improving power/spectral efficiency. IM extends the constellation symbol space by mapping extra information bits to the indices of the building blocks of the communication system, in addition to the bits traditionally carried by the complex symbols. As such, the spectral efficiency can be improved without involving more power consumption. Capitalizing on the enhancements brought by the IM concept, it has been studied under different systems, such as orthogonal frequency division multiplexing (OFDM) [8], wireless sensor networks [9], cooperative networks [10] and to the polarization of signals [11].

Recently, the concept of IM has been introduced to multiuser scenarios, where a novel uplink MA called IM-based MA (IMMA) is proposed in [12]. In IMMA, each user activates a single channel using part of its bit block and modulates the remaining part as a complex symbol emitted over the activated channel. Thus, the spectral efficiency is improved by delivering extra information bits carried by the index of the active channel for each user. Despite of the potential data collision among users, it is shown that the achievable BER in IMMA outperforms OMA and SCMA schemes [12]. However, the adopted detection algorithm in IMMA is based on ML which suffers from high computational complexity. In [13], the indexing space of IMMA is extended by activating multiple channels under OFDMA system which led to a more spectral-efficient scheme. In [14], Quadrature IMMA (QIMMA) approach is proposed to extend the indexing space, and hence to improve the spectral efficiency of IMMA, where a user activates two independent channels, one for the real part and the other for the imaginary part of the modulated symbol. It is worth mentioning that all of the

above discussed IM-based MA schemes are designed for uplink only and suffer from poor performance in the downlink. More recently, a downlink scheme was proposed in [15], where the case of only two users is considered in which the near user applies OFDM, i.e., occupies all of the available subcarriers, whereas the far user applies OFDM-IM as in [8]. Thus, the signals of both users are multiplexed in power domain following the NOMA concept. However, this scheme fits for the two users' case only.

1.2 Thesis Objectives

The objective of this research is to establish an understanding on the different multiple access techniques in the literature such as OMA, NOMA and the IM-based multiple access techniques. In addition to proposing an efficient and flexible multiple access method based on the IM concept.

In this thesis, building on the appealing enhancements brought by the IM and NOMA and the aforementioned opportunity in the literature, a novel downlink MA scheme called IM based NOMA (IM-NOMA) is proposed. Specifically, the bit block to be sent to each user is divided into two subblocks. The first sub-block is mapped to a complex symbol drawn from M-ary constellation, while the second sub-block is used to index a set of channels, each of which will carry a replicated copy of the modulated symbol. Consequently, as in NOMA, modulated symbols are scaled by different power levels according to their channel gains, and then symbols to be sent over the same channel are superimposed in one signal. It is noteworthy that the extra bits carried by the indexing bits improve the per-user spectral efficiency, while sending multiple copies over multiple independent channels improves the transmit diversity. To establish a performance benchmark, a closed form upper bound expression on the average bit error rate (BER) of IM-NOMA is derived considering Rayleigh fading channel for ML detection, while an approximation is provided for the

SIC detection case. Simulation results under different setups confirm the significant enhancement of the proposed scheme in terms of BER performance as compared to classical PD-NOMA and the related schemes in the literature.

The contributions of this work can be summarized as follows:

- A novel IM-based NOMA scheme is proposed that leverage the power efficiency and flexibility of IM and the spectral efficiency of NOMA.
- The error performance of the proposed scheme is analyzed under two detection schemes, namely ML and SIC, considering Rayleigh fading channels.
- The computational complexity of the proposed scheme is studied and compared with that of PD-NOMA.
- A simple low complexity detection method is proposed for the case of two users, based on the constellation rotation concept.
- The outage probability of the proposed scheme is derived in a closed-form formula for both detection schemes. In addition, the diversity gain is studied for the SIC detection case.
- Numerical simulations are provided to validate the analytical findings and to show the superiority of the proposed scheme over the conventional PD-NOMA and the recently proposed IM-based NOMA schemes.

1.3 Thesis Outline

This thesis is organized as follows: The literature review is presented in Chapter 2, where we survey the most recent IM-based and SM-based multiple access techniques. The conventional PD-NOMA scheme is investigated in Chapter 3, where

a novel closed form expressions for the BER performance and diversity gain under ML and SIC detection are provided. The proposed IM-NOMA scheme is presented in Chapter 4, where we start by the signal and channel models followed by the derivations of its error and outage performance under two detection methods, namely ML and SIC. In Chapter 5, the numerical and simulation results are shown, where the proposed scheme is compared to the classical PD-NOMA as well as with two of the related, recently proposed, schemes. Finally, concluding remarks and insights are drawn in Chapter 6.

CHAPTER 2: LITERATURE REVIEW

A comprehensive literature review is reported in this chapter covering the most recent IM-based and SM-based multiple access techniques.

2.1 IM-based Multiple Access Schemes

Adopting IM in the context of multiple access scenarios has been recently introduced in [12, 14], where different variants of uplink multiple access schemes have been proposed and analyzed. However, those schemes show good performance only in the uplink scenario as discussed in the background section. Recently, two related schemes were proposed considering the case of two users [15, 16]. In both schemes, the near user applies OFDM by occupying all available subcarriers, while OFDM-IM [8] is applied by the far user. Moreover, [15] considers the downlink case while the scheme in [16] is proposed for the uplink scenarios. Thus, adopting PD-NOMA concept, power domain multiplexing is done for the users' signals. Detection computational complexity arises as an inherited drawback when adopting IM concept in any communications system. A log likelihood ratio (LLR)-based detection algorithm was proposed in [17], where it is shown that it achieves near optimal performance while maintaining a relatively low complexity as compared to ML detection. Another low complexity detection method was proposed in [18] based on the constellation rotation, and was shown to significantly reduce the SIC complexity for the case of two users. A similar IM-aided NOMA scheme was proposed in [19] for visible light communications (VLC), where users are clustered in pairs. For each pair, one user is served using conventional OFDM, and data of the other is conveyed using IM-based on-off keying concept. More recently, a combination of IM and uplink NOMA was studied in [20, 21], where both proposed schemes fit for the case of two users in the uplink direction. Furthermore, in [21] a cooperative NOMA is considered where one of the users plays the role of a relay to forward messages to the second

user. Spatial modulation (SM) [22] is considered as a special case of IM, where the indices of the transmit antennas are used to convey the extra information to the receiver. In this context, few works have considered the integration between SM and NOMA [23, 24]. In [23], SM was applied in a MIMO system where a single antenna is activated per user, and power allocation scheme is applied to mitigate the inter-user interference. A similar scheme was proposed in [24], in which cooperative NOMA is assumed and the case of two users only is considered. It is worth mentioning here that all multi-user SM-based systems suffer from high cost and low power efficiency due to having high number of RF chains [25]. For instance, in downlink SM-based communications, the number of required RF chains should be at least equal the number of served users. However, few works, [26, 27], have proposed a modified SM-NOMA schemes, utilizing a single RF chain, to improve power efficiency and reduce hardware implementation complexity. Nevertheless, those schemes are applicable to the case of two users only, where the spatial bits are transmitted to one user and the complex modulated symbols are transmitted to the other user.

A more similar downlink IM-NOMA scheme has been proposed recently in [28]. However, it considers only the simplified case of two users in the system model and the derivation of the error performance under the SIC detection. Furthermore, the interference between users is neglected in the derivation which might give acceptable analytical results in the two users' case. For the general case, it is expected to result in a loose bound on the performance as the number of users increases. Moreover, the error performance under SIC detection is the only investigated metric in this work while investigating other metrics such as the outage probability and the diversity gain of such systems (as considered in this thesis) is important to give more insights on newly proposed schemes.

As seen in the above discussion, the related works assume special cases which limit the flexibility of the proposed scheme. Specifically, the case of only two users has been considered in [15]-[16], [19]-[21], [24], [26]-[28], with a limited analytical performance analysis. In [15]-[16], only one user applies IM-OFDM while the second user applies NOMA-OFDM. Only the uplink transmission scenario has been adopted in [12]-[14], [16], [20]-[21]. Finally, in [21] and [24], a cooperative scenario is assumed where a user functions as a relay for the other user. Clearly, a system under these assumptions cannot be generalized, and will suffer from inflexibility especially when adopting more complicated cases such as multiple non-cooperative users, general power allocation method and/or different subcarrier activation ratio per user. In this thesis, leveraging the advantages of both the IM and NOMA schemes, and targeting the explained gap in the available literature, a new downlink multiple access scheme called index-modulation based NOMA (IM-NOMA) is proposed. The proposed scheme implies that the base station (BS) selects the subcarrier(s) over which the signal of a user is transmitted based on part of its data, employing the IM principle. Additionally, the BS divides the total transmit power among users following the NOMA principle, where the allocated power level for a user is inversely proportional to its channel conditions. Such a novel scheme can leverage the benefits of both IM and NOMA to present a flexible and enhanced downlink scheme in terms of the error performance and the number of served users.

CHAPTER 3: NOMA ERROR PERFORMANCE

In this chapter, the system model of conventional PD-NOMA system is presented, with our contributions on deriving the BER closed form formulas for two common detection methods, namely ML and SIC. More specifically, the average pairwise error probability (PEP) is derived for downlink NOMA systems considering that power is allocated based on the distance of the corresponding user. The derived PEP is obtained under Nakagami-m fading channels, where Rayleigh fading case can be easily obtained as a special case. Moreover, the two detection techniques are considered with any number of users and modulation order. Finally, the derived PEP is used to obtain the diversity gain and an upper bound on the average BER. The results presented in this chapter are published in [29].

3.1 System Model

The considered system model consists of N users that are being served by a single BS. In NOMA, users to be served by the same resources are selected in such a way to have a sparse distribution within the coverage area of the BS. Users are assumed to be located at different distances from the BS. The distance between the n^{th} $(1 \leq n \leq N)$ user and the BS is denoted by d_n, where $d_1 < d_2 < \cdots < d_N$. Based on the users' distances, the BS allocates different power levels. Specifically, the power allocated to user n, is denoted by p_n where $p_1 < p_2 < \cdots < p_N$. Considering the limited power budget at the BS, the total power allocated to users should sum up to P_t, the total available power at the BS. The static transmit power allocated to user n is given by $p_n = \rho_n P_t$, where $0 < \rho_n \leq 1$ represents the power portion allocated to user n and is given as [30]

$$\rho_n = \frac{d_n^2}{\sum_{i=1}^{N} d_i^2}, \tag{1}$$

where d_n is the distance between user n and the BS.

The signals to be sent to the N users are weighted by their corresponding power levels and superimposed to obtain the transmitted signal x that is given as

$$x = \sum_{n=1}^{N} \sqrt{\rho_n} s_n, \tag{2}$$

where s_n represents the complex baseband symbol to be transmitted to user n. The received signal at user n, denoted by y_n, can be expressed as follows

$$y_n = \sqrt{P_t d_n^{-\eta}} h_n \left(\sum_{i=1}^{N} \sqrt{\rho_i} s_i \right) + w_n, \tag{3}$$

where η is the path loss exponent, h_n is the instantaneous complex channel fading between the BS and user n, and w_n is the additive white complex Gaussian noise $w_n \sim \mathcal{CN}(0, \sigma^2)$.

In all detection methods, it is assumed that a user is aware of its instantaneous channel gain with the BS, i.e., h_n, and the set of the power coefficients of all users, i.e., ρ_i for $i = 1, \dots, N$. In the following we consider two detection techniques, namely: ML and SIC.

3.2 ML Detection

ML represents the optimal detection method, where each user jointly detects the signals of all users at once. Let us define the vector $s = [s_1, s_2, \cdots, s_N]$ which includes the transmitted signals for all users. Notice that the vector s has 2^{NB} different candidate forms, where B is the number of transmitted bits for each user. The ML detection works as follows

$$\hat{\boldsymbol{s}} = \arg \min_{j=1:2^{NB}} \left| y_n - \sqrt{p_{r,n}} h_n x^{(j)} \right|^2, \tag{4}$$

where $p_{r,n} = P_t d_n^{-\eta}$ is the average received power at user n, and $x^{(j)}$ is the superimposed signal, obtained based on (2), if the vector s_j is sent from the BS.

Despite of its optimal performance, ML is considered as the most computationally complex method. Considering the number of real multiplications as a measure of the computational complexity, each user requires 2^{NB+3} real multiplications.

3.3 SIC Detection

In SIC detection method, a user starts by decoding the signals of the users that are farther than him, one by one. Each detected signal is subtracted from the received signal, and the resulting signal is considered as the received signal to be decoded for the next user. The detection process is repeated till a user reaches its own signal. As such, the number of signals to be decoded by a user depends on its distance from the BS with respect to other users' distances. The farthest user decodes its signal only, while the nearest user decodes all users' signals one by one.

Considering user n, its decoded signal $\widehat{s_n}$ is detected as follows

$$\widehat{s_n} = \arg \min_{j=1:2^B} \left| y_n - \sqrt{p_{r,n}} h_n \left(\sum_{k=n+1}^{N} \sqrt{\rho_k}\, \widehat{s_k} \right) - \sqrt{p_{r,n}\rho_n} h_n s^{(j)} \right|^2, \qquad (5)$$

where $s^{(j)}$ represents the j^{th} candidate symbol transmitted from the BS to user n. The second term in (5) represents the subtracted signals of the users farther than the n^{th} user.

It is clear that the computational complexity induced by SIC varies for each user based on its distance from the BS. Specifically, the farthest user has the least computational complexity, where it requires only $(3 + 2^{B+2})$ real multiplications. On

the other hand, the nearest user has the highest computational complexity, where it requires $N(3+2^{B+2})$ real multiplications.

3.4 BER Analysis

In this section, the BER performance of NOMA in the downlink is analyzed for both detection rules. Specifically, the pairwise error probability is derived in closed form expression based on both methods, which is then used to obtain an upper bound on the average BER.

In general, the average BER of user n in decoding its own symbol is expressed using the union bounding technique as follows

$$\mathrm{BER}_n = \frac{1}{2^{NB}\log_2 M}\sum_{i=1}^{2^{NB}}\sum_{j=1}^{2^{NB}}\tau_{ij}\mathrm{PEP}_{i,j}, \tag{6}$$

where τ_{ij} represents the Hamming distance, i.e., the number of different bits, between the considered pair (i,j).

3.4.1 ML Detection Error Performance

According to (3), the $\mathrm{PEP}_{i,j}$ can be expressed as

$$PEP_{i,j} = Pr.\left\{\left|y_n - \sqrt{p_{r,n}}h_n x^{(j)}\right|^2 > \left|y_n - \sqrt{p_{r,n}}h_n x^{(i)}\right|^2\right\}. \tag{7}$$

As $x^{(j)}$ is the actual transmitted signal, (7) can be simplified as

$$\mathrm{PEP}_{i,j} = \Pr.\left\{|w_n|^2 > \left|\sqrt{p_{r,n}}h_n\Delta_{ji} + w_n\right|^2\right\}, \tag{8}$$

where $\Delta_{j,i} = x^{(j)} - x^{(i)}$. The PEP conditioned on h_n can be expressed as follows

$$\mathrm{PEP}_{i,j|h_n} = Q\left(\sqrt{\frac{p_{r,n}|h_n|^2\left|\Delta_{ji}\right|^2}{2\sigma^2}}\right) \tag{9}$$

where its average (unconditional) value can be computed by integrating over the probability density function (pdf) of $|h_n|^2$, denoted by $f_{|h_n|^2}(\gamma)$, as follows

$$\mathrm{PEP}_{i,j} = \int_0^{\infty} Q\left(\sqrt{\Omega_{ij}\gamma}\right) f_{|h_n|^2}(\gamma) d\gamma, \tag{10}$$

where Ω_{ij} is given as

$$\Omega_{ij} = \frac{p_{r,n}\left|\Delta_{ji}\right|^2}{2\sigma^2}. \tag{11}$$

For Nakagami-m fading model, $|h_n|^2$ is a gamma random variable [31], and hence, by substituting the PDF of Gamma distribution in (10), and using the Craig formula of the Q-function [32] it can be rewritten as follows

$$\mathrm{PEP}_{i,j} = \frac{m^m}{\Gamma(m)\pi} \int_0^{\frac{\pi}{2}} \int_0^{\infty} exp\left(-\left(\frac{\Omega_{ij} + 2m\sin^2\theta}{2\sin^2\theta}\right)\gamma\right)\gamma^{m-1}\, d\gamma d\theta. \tag{12}$$

Furthermore, the inner integral in (12) can be solved using equation (3.381.4) from [33] to yield

$$\mathrm{PEP}_{i,j} = \frac{1}{\pi} \int_0^{\frac{\pi}{2}} \left(\frac{\sin^2\theta}{\frac{\Omega_{ij}}{2m} + \sin^2\theta}\right)^m d\theta, \tag{13}$$

which can be solved in turn in a closed form expression using equation (64) from [31] as follows

$$\mathrm{PEP}_{i,j} = \left(\chi_{ij}\right)^m \sum_{t=0}^{m-1} \binom{m-1+t}{t} \left(1-\chi_{ij}\right)^t, \tag{14}$$

where χ_{ij} is given as

$$\chi_{ij} = \frac{1}{2}\left(1 - \sqrt{\frac{\Omega_{ij}}{2m+\Omega_{ij}}}\right). \tag{15}$$

As a special case, the average PEP over Rayleigh fading channel can be obtained by setting $m = 1$ in (14).

3.4.2 SIC Detection Error Performance

For user n, the PEP that it erroneously decodes its own symbol as $s^{(i)}$ given that $s^{(j)}$ was actually sent, can be expressed as follows

$$PEP_{i,j} = Pr.\left\{\left|\hat{y}_n - \sqrt{p_{r,n}\rho_n}h_n s^{(j)}\right|^2 > \left|\hat{y}_n - \sqrt{p_{r,n}\rho_n}h_n s^{(i)}\right|^2\right\}, \quad (16)$$

where $\hat{y}_n$ represents the received signal after subtracting the detected contributions from the farther users, and is given as

$$\hat{y}_n = y_n - \sqrt{p_{r,n}\rho_n}h_n\left(\sum_{k=n+1}^{N}\sqrt{\rho_k}\hat{s}_k\right) \quad (17)$$

As $s^{(j)}$ is actually transmitted, (16) can be rewritten as

$$\begin{aligned} PEP_{i,j} = Pr.\Big\{&\left|\sqrt{p_{r,n}}h_n r_n + w_n\right|^2 \\ &> \left|\sqrt{p_{r,n}}h_n\left(\sqrt{\rho_n}\delta_{ji} + r_n\right) + w_n\right|^2\Big\}, \end{aligned} \quad (18)$$

where $\zeta_k = s_k - \hat{s}_k$, $\delta_{ji} = s^{(j)} - s^{(i)}$, and r_n is given as

$$r_n = \left(\sum_{k=n+1}^{N}\sqrt{\rho_k}\zeta_k + \sum_{k=1}^{n-1}\sqrt{\rho_k}s_k\right). \quad (19)$$

Equation (18) can be written in terms of Q function after conditioning on the channel h_n and expanding the squared norms and rearranging to yield

$$PEP_{i,j|h_n} = Q\left(\sqrt{\omega_{ij}^2|h_n|^2}\right), \quad (20)$$

where ω_{ij} is given as

$$\omega_{ij} = \frac{\sqrt{p_{r,n}\rho_n}\left|\delta_{ij}\right|^2 + 2\sqrt{p_{r,n}}\mathcal{R}(r_n^*\delta_{ij})}{\sqrt{2\left|\delta_{ij}\right|^2\sigma^2}}, \quad (21)$$

Where $\mathcal{R}(z)$ returns the real part of z.

Finally, the unconditional PEP can be computed by following the same steps in (9)-(14), which gives the same expression as in (14) while replacing Ω_{ij} by ω_{ij}^2 in (15).

3.4.3 Asymptotic PEP

The conditional PEP at user n, given in (9), can be upper bounded by using Chernoff bound as follows

$$\mathrm{PEP}_{i,j|h_n} \leq \exp\left(-\frac{\gamma_n^2\left|\Delta_{ij}\right|^2}{2}\right), \tag{22}$$

where $\gamma_n^2 = \frac{P_t d_n^{-\eta}|h_n|^2}{2\sigma_n^2}$ denotes the instantaneous received SNR at user n. Hence, the asymptotic unconditional PEP can be obtained by averaging (22) over the PDF of γ_n^2, which is a Gamma distribution, as follows

$$\mathrm{PEP}_{i,j} \leq \frac{m^m}{\bar{\gamma}_{\mathrm{n}}^{\mathrm{m}}\Gamma(m)} \int_0^\infty \gamma_n^{m-1} \exp\left(-\left(\frac{\left|\Delta_{ij}\right|^2}{2} + \frac{m}{\bar{\gamma}_n}\right)\gamma_n\right) d\gamma_n, \tag{23}$$

where $\bar{\gamma}_n$ is the average SNR at user n.

The integral in (23) can be solved using equation (3.381.4) from [33] as follows

$$\mathrm{PEP}_{i,j} \leq \left(\frac{2m}{\bar{\gamma}_{\mathrm{n}}\left|\Delta_{\mathrm{ij}}\right|^2 + 2\mathrm{m}}\right)^m. \tag{24}$$

The diversity gain is defined as follows

$$d_s = \lim_{\bar{\gamma}_n \to \infty} -\frac{\log\left(\mathrm{PEP}_{ij}\right)}{\log(\bar{\gamma}_n)}, \tag{25}$$

which can be rewritten by substituting (24) as follows

$$d_s = \lim_{\bar{\gamma}_n \to \infty} -\frac{m\log(2m)}{\log(\bar{\gamma}_n)} + \frac{m\log\left(\bar{\gamma}_n|\Delta_{ij}|^2 + 2m\right)}{\log(\bar{\gamma}_n)}. \tag{26}$$

As $\bar{\gamma}_n \to \infty$, the first term approaches zero, while $\log\left(\overline{\gamma_n}|\Delta_{ij}|^2 + 2m\right) \approx \log\left(\overline{\gamma_n}|\Delta_{ij}|^2\right)$. Consequently, (26) can be simplified to

$$d_s \approx \lim_{\bar{\gamma}_n \to \infty} \frac{m \log\left(\bar{\gamma}_n |\Delta_{ij}|^2\right)}{\log(\bar{\gamma}_n)} \approx m. \tag{27}$$

It is worth noting here that the diversity gain (27) is valid for both detection methods and, unlike the result in [34], the diversity gain is identical for all users. This is due to the assumption that all users suffer from identical (independent) small-scale fading.

CHAPTER 4: THE PROPOSED IM-NOMA SCHEME

4.1 System Model

The considered system consists of N_T users that are being served by a single BS. The total bandwidth dedicated for the downlink data transmission, denoted by B_T, is divided into L_T orthogonal subcarriers each of B_c bandwidth, as in conventional orthogonal frequency division multiple access (OFDMA) systems. Each L adjacent subcarriers are grouped into a chunk which is dedicated to serve $N \leq N_T$ users.

In the proposed IM-NOMA scheme [35, 36], the BS delivers B bits for each user at each transmission time. For the n^{th} user ($1 \leq n \leq N$), the B bits are divided into two blocks. The first block, which includes $log2(M)$ bits, is passed through a MPSK modulator and mapped to a complex symbol denoted by c_n, while the second block, which includes $\left\lfloor log2\binom{L}{K} \right\rfloor$ bits ($1 \leq K \leq L$), specifies a combination of K subcarriers within the chunk L to carry the modulated symbol c_n, as shown in Figure 1.

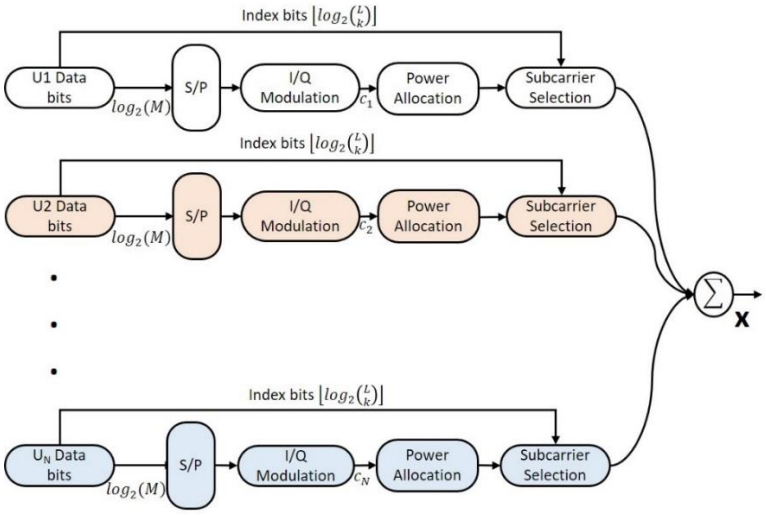

Figure 1. IM-NOMA System Model.

Accordingly, the transmitted signal to user n on subcarrier ℓ is given as follows

$$s_{n\ell} = \begin{cases} c_n; \ell \in \hat{\ell}_n \\ 0; \ell \notin \hat{\ell}_n \end{cases} \quad (28)$$

where $\hat{\ell}_n$ is the n^{th} user's set of selected subcarriers' indices. The same procedure is performed for each user to determine the modulated symbol and the active subcarriers for each user. As in conventional NOMA scheme, modulated symbols to different users on the same subcarrier will be superimposed and transmitted at once. However, different power levels are allocated to different users based on their distances from the BS. Specifically, the signal to user n will be scaled by the coefficient ρ_n computed as follows [30]

$$\rho_n = \frac{d_n^2}{\sum_{i=1}^{N} d_i^2} \quad (29)$$

where d_n is the distance between user n and the BS. There are different power allocation methods in the literature based on the availability of the CSI, where the power allocation and user pairing can be done based on the users' distances [37] or based on their instantaneous channel gains [38, 39]. It is worth noting that the objective of this work is to propose an efficient and flexible scheme, hence a simple power allocation method is adopted. Further studies can be done to investigate the optimal power allocation and user pairing options. Moreover, the pairwise error probability (PEP) derivation in the following subsection is independent of the power allocation in (29), and hence it holds for other power allocation methods.

Thus, the transmitted signal from the BS to all users over subcarrier ℓ, denoted by x_ℓ, can be expressed as

$$x_\ell = \sum_{i=1}^{N} \sqrt{\rho_n} s_{n\ell} \quad (30)$$

At user n, the received signal from the BS over subcarrier ℓ is expressed as follows

$$y_{n\ell} = \sqrt{P_{r,n}} h_{n\ell} x_{\ell} + \omega_{n\ell} \tag{31}$$

where $P_{r,n} = P_t d_n^{-\eta}$ represents the received power at user n, P_t is the total transmitted power, η is the path loss exponent, $h_{n\ell}$ denotes the channel between user n and the BS over subcarrier ℓ, and $\omega_{n\ell} \sim \mathcal{CN}(0, \sigma_{\mathrm{n}}^2)$ is the additive white Gaussian noise at the receiver input of user n over subcarrier ℓ. Without loss of generality, the channel coefficients between the BS and the users are modeled as independent and identically distributed (i.i.d) Rayleigh flat fading channels.

In what follows, ML and SIC detection methods are considered to jointly decode the transmitted indexing and complex modulated bits for each user.

4.1.1 Maximum Likelihood Detection

In this detection technique, each user jointly decodes the transmitted signals for all users. Define the vector $\boldsymbol{y}_n = [y_{n1}, y_{n2}, \dots, y_{nL}]$ to represent the received signals at user n over all subcarriers in its corresponding chunk, and the vector $\boldsymbol{x}_n = [x_1, x_2, \dots, x_L]$ to represent the transmitted signals from the BS over all subcarriers in the corresponding chunk. Accordingly, (31) can be rewritten in a matrix form as

$$\boldsymbol{y}_n = \sqrt{P_{r,n}} \boldsymbol{h}_n \odot \boldsymbol{x} + \boldsymbol{w}_n \tag{32}$$

where $\boldsymbol{h}_n = [h_{n1}, h_{n2}, \dots, h_{nL}]^T$, $\odot$ is the Hadamard product, i.e., element-wise product, and $\boldsymbol{w_n} = [\omega_{n1}, \omega_{n2}, \dots, \omega_{nL}]^T$.

At user n, ML detection can be applied to detect the received signals of all users at once as follows

$$\hat{\boldsymbol{x}} = \arg \min_{\boldsymbol{x}^{(i)} \in \mathcal{X}} \left\| \boldsymbol{y}_n - \sqrt{P_{r,n}} \boldsymbol{h}_n \odot \boldsymbol{x}^{(i)} \right\|^2 \tag{33}$$

where $\|\cdot\|^2$ is the squared Euclidean norm, and $\mathcal{X}$ is the set of all possible transmitted vectors $\boldsymbol{x}$. It is worth mentioning that the set $\mathcal{X}$ includes 2^{NB} different candidate transmission vectors that should be tested in ML detection. As such, despite its optimal performance, ML detection induces a high computational complexity which might not be affordable, especially at large values of N, L and/or M.

4.1.2 Successive Interference Cancellation Detection (SIC)

SIC detection is considered as a good alternative to reduce the high computational complexity of the ML technique at the cost of a slight performance degradation. In SIC, each user should decode and cancel the signals of the users that are farther than him. Specifically, user n will first detect the signal vector of user N, s_N, (the farthest user from the BS) assuming all other signals as noise. The detected signal vector s_N will then be subtracted from the received signal vector. The same procedure is repeated till user n extracts its own signal. Note that the first user, i.e., the closest user, needs to cancel the signals of all other users, while user N, the farthest user, does not cancel any signal and directly detects its signal treating other users' signals as noise, as shown in Figure 2.

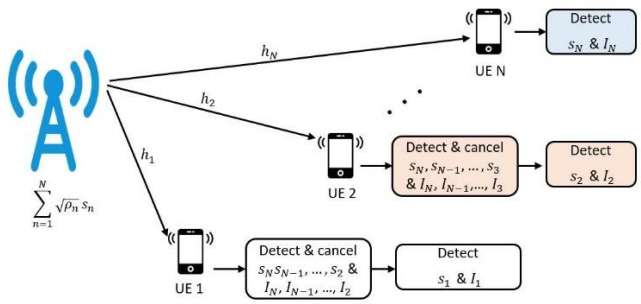

Figure 2. IM NOMA with SIC Detection Block Diagram.

Mathematically, user n will detect its own signal vector as follows

$$\hat{\boldsymbol{s}}_n = \arg \min_{\boldsymbol{s}_n^{(i)} \in \mathcal{S}_n} \left\| \boldsymbol{y}'_n - \sqrt{P_{r,n}\rho_n}\boldsymbol{h}_n \odot \boldsymbol{s}_n^{(i)} \right\|^2 \tag{34}$$

where $\mathcal{S}$ is the set of all possible transmitted vectors to a user, and $\boldsymbol{y}'_n$ represents the received signal after cancelling the farther users' signals and is defined as

$$\boldsymbol{y}'_n = \boldsymbol{y}_n - \sqrt{P_{r,n}}\boldsymbol{h}_n \odot \left(\sum_{i=n+1}^{N} \sqrt{\rho_i}\hat{\boldsymbol{s}}_i \right) \tag{35}$$

4.2 Error Performance Analysis

In the following subsections, the pairwise error probability (PEP) considering both detection techniques, ML and SIC, is derived. Where a closed form expression is derived for the ML case while an approximation is provided for the SIC counterpart. Then, the bit error rate's (BER) upper bound is obtained by employing the union bounding technique.

4.2.1 ML Detection Error Performance

As per the union bounding method [40], the upper bound on the BER at user n is expressed in terms of the PEP as follows

$$\mathrm{BER}_n = \frac{1}{2^{NB}B} \sum_{\substack{i=1,\dots,2^{NB} \\ j=1,\dots,2^{NB}}} \tau_{ij,n}\mathrm{PEP}_{ij} \tag{36}$$

with $\tau_{ij,n}$ representing the distance in terms of the number of different bits between the pair (i, j) under consideration, and PEP_{ij} is the PEP, which simply measures the likelihood of erroneously detecting the vector $\boldsymbol{x}^{(i)}$ while the transmitted vector is actually $\boldsymbol{x}^{(j)}$. Hence, incorporating (33), the PEP is rewritten as follows

$$\mathrm{PEP}_{ij} = \Pr\left\{ \left\| \boldsymbol{y}_n - \sqrt{p_{r,n}}\boldsymbol{h}_n \odot \boldsymbol{x}^{(j)} \right\|^2 > \left\| \boldsymbol{y}_n - \sqrt{p_{r,n}}\boldsymbol{h}_n \odot \boldsymbol{x}^{(i)} \right\|^2 \right\}. \tag{37}$$

Now, since the vector $\boldsymbol{x}^{(j)}$ was actually transmitted and by substituting (32), (37) can be simplified to be

$$\mathrm{PEP}_{ij} = \Pr\left\{\|\boldsymbol{w}_n\|^2 > \left\|\sqrt{p_{r,n}}\boldsymbol{h}_n \odot \boldsymbol{\Delta}_{\mathrm{ji}} + \boldsymbol{w_n}\right\|^2\right\}. \tag{38}$$

where $\boldsymbol{\Delta}_{ji} = \boldsymbol{x}^{(j)} - \boldsymbol{x}^{(i)}$. Next, the conditional PEP can be written in terms of the Q function, for a given channel instance, as follows

$$\mathrm{PEP}_{ij|\boldsymbol{h}_n} = \mathrm{Q}\left(\sqrt{\frac{\psi_{ji,n}}{2\sigma_n^2}}\right), \tag{39}$$

where $\psi_{ji,n} = \left\|\sqrt{p_{r,n}}\boldsymbol{h}_n \odot \boldsymbol{\Delta}_{ji}\right\|^2 = p_{r,n}\sum_{\ell=1}^{L}|h_{n\ell}\delta_\ell|^2$, and δ_ℓ is the ℓ^{th} element in $\boldsymbol{\Delta}_{ji}$. Given that $\boldsymbol{h}_{n\ell} \sim \mathcal{CN}(0,1)$, ψ_{ji} is a sum of L exponential random variables (RVs), where the mean of the ℓ^{th} RV is $\mu_\ell = p_{r,n}|\delta_\ell|^2$. Actually, there are $K \leq L$ RVs having nonzero means. Furthermore, there are R out of K RVs having unique means $\mu_1, \mu_2 \cdots, \mu_R$. Let us denote the number of RVs with the mean μ_i as r_i. Therefore, the PDF of $\psi_{ji,n}$ is given in equation (9) in [41] as follows

$$\mathrm{f}_{\psi_{ji,n}}(\varphi) = \sum_{\mathrm{q}=1}^{\mathrm{R}} \lambda_q^{r_q} e^{(-\lambda_q\varphi)} \sum_{\omega=1}^{r_q} A_{q,\omega}\frac{(-1)^{r_q-\omega}}{(\omega-1)!}\varphi^{\omega-1}, \tag{40}$$

where $A_{q,\omega} = \sum_{\substack{m_1+\cdots+m_R=r_q-\omega \\ m_q=0}} \prod_{\substack{t=1 \\ t\neq q}}^{R}\binom{r_t+m_t-1}{m_t}\frac{\lambda_t^{r_t}}{(\lambda_t-\lambda_q)^{r_t+m_t}}$ and $\lambda_\ell = \frac{1}{\mu_\ell}$.

Then, by integrating (39) over the PDF given in (40) and following the same steps in [12] we get

$$\mathrm{PEP}_{i,j} = \sum_{\mathrm{q}=1}^{\mathrm{R}} \lambda_q^{r_q} \sum_{\omega=1}^{r_q} A_{q,\omega}(-1)^{r_q-\omega}\frac{\chi_q}{\lambda_q}\sum_{p=0}^{\omega-1}\binom{\omega-1+p}{p}(1-\chi_q)^p, \tag{41}$$

where $\chi_q = \frac{1}{2}\left(1 - \frac{1}{\sqrt{1+4\sigma^2\lambda_q}}\right)$. A more detailed derivation can be found in our paper [42].

4.2.2 SIC Detection Error Performance

Unlike the case in ML detection, in SIC each user retrieves its own data only after cancelling the interfering signals from other users. Therefore, considering user n, $\mathrm{PEP}_{ij,n}$ can be expressed as

$$\mathrm{PEP}_{ij,n} = \Pr\left\{\left\|\boldsymbol{y}'_n - \sqrt{p_{r,n}\rho_n}\boldsymbol{h}_n \odot \boldsymbol{s}_n^{(j)}\right\|^2 > \left\|\boldsymbol{y}'_n - \sqrt{p_{r,n}\rho_n}\boldsymbol{h}_n \odot \boldsymbol{s}_n^{(i)}\right\|^2\right\}. \quad (42)$$

Eq. (42) can be formulated in terms of the Q function after some simple mathematical manipulations to yield the following

$$\mathrm{PEP}_{ij,n|\boldsymbol{h}_n} = \mathrm{Q}\left(\sqrt{\frac{p_{r,n}(\|\boldsymbol{g}_n\|^2 - \boldsymbol{g}_n^*\boldsymbol{t}_n)^2}{2\|\boldsymbol{g}_n\|^2\sigma_n^2}}\right), \quad (43)$$

where $\boldsymbol{g}_n = \boldsymbol{h}_n \odot \boldsymbol{b}_n$, $\boldsymbol{t}_n = \boldsymbol{h}_n \odot \boldsymbol{r}_n$, $\boldsymbol{b}_n = \boldsymbol{s}_n^{(i)} - \boldsymbol{s}_n^{(j)}$, $\boldsymbol{r}_n = \sum_{k=n+1}^{N}\sqrt{\rho_k}\boldsymbol{e}_k + \sum_{k=1}^{n-1}\sqrt{\rho_k}\boldsymbol{s}_k^{(i)}$, and $\boldsymbol{e}_k = \boldsymbol{s}_k^{(i)} - \boldsymbol{s}_k^{(j)}$. Such an equation cannot be mathematically tackled due to including rational correlated random variables that cannot be reduced. However, an approximation can be made for user N (the worst channel). As the user N has the highest power coefficient, we can assume that the values of other power coefficients are neglected. As such, $\boldsymbol{r}_n \approx \boldsymbol{0}$, and hence, $\boldsymbol{t}_n \approx \boldsymbol{0}$. Accordingly, (43) can be approximated for user N to yield

$$\mathrm{PEP}_{ij,N|\boldsymbol{h}_n} \approx \mathrm{Q}\left(\sqrt{\frac{p_{r,N}\|\boldsymbol{g}_N\|^2}{2\sigma_n^2}}\right) = \mathrm{Q}\left(\sqrt{\frac{\psi'_{ji,N}}{2\sigma_n^2}}\right), \quad (44)$$

which can be solved using the same procedure in (39)-(41) to yield the same formula in (41) with replacing λ_q by $\lambda'_q = \frac{1}{\mu'_q}$, where $\mu'_\ell = p_{r,N}|\delta'_\ell|^2$ and δ'_ℓ is the ℓ^{th} element in $\boldsymbol{b}_N$.

4.3 Outage Probability Analysis

In the following subsections, outage probability expressions are derived in closed-form expressions for both detection methods. Furthermore, the asymptotic diversity gain is derived for the SIC detection technique.

4.3.1 ML Detection Outage Probability

Considering the received signal at user n as in (31), the received instantaneous SNR can be expressed as follows

$$\text{SNR}_n = \frac{\left\|\sqrt{p_{r,n}}\boldsymbol{h}_n \odot \boldsymbol{x}\right\|^2}{\sigma_n^2}. \tag{45}$$

The outage probability at user n, denoted by $P_{o,n}$, can be written as

$$P_{o,n} = \Pr\{\text{SNR}_\text{n} < \gamma_\text{th}\}, \tag{46}$$

where γ_th denotes a given SNR threshold. Then, the outage probability $P_{o,n}$, using (46), can be written as follows

$$P_{o,n} = \Pr\left\{\left\|\sqrt{p_{r,n}}\boldsymbol{h}_n \odot \boldsymbol{x}\right\|^2 < \gamma_\text{th}\sigma_n^2\right\}, \tag{47}$$

which can be simplified, after expanding the norm and rearranging, to yield

$$P_{o,n} = \Pr\left\{\sum_{\ell=1}^{L}|h_{n\ell}|^2\,(\rho_n|s_{n\ell}|^2) < \frac{\gamma_\text{th}\sigma_n^2}{p_{r,n}}\right\}. \tag{48}$$

Consequently, the outage probability is the cumulative distribution function (CDF) of (40) evaluated at $\frac{\gamma_{\text{th}}\sigma_n^2}{p_{r,n}}$, which can be derived using equation 3.381.1 in [33] to yield

$$\mathrm{P}_{o,n} = \sum_{\mathrm{q}=1}^{\mathrm{R}} \lambda_q^{r_q} \sum_{\omega=1}^{r_q} A_{q,\omega} \frac{(-1)^{r_q-\omega}}{(\omega-1)!} \left(\frac{1}{\lambda_q}\right)^{\omega} \gamma\left(\omega, \lambda_q \frac{\gamma_{\text{th}}\sigma_n^2}{p_{r,n}}\right), \tag{49}$$

Where $A_{q,\omega}$ is defined as in (41), $\lambda_\ell = \frac{1}{\rho_n |s_{n\ell}|^2}$ and $\gamma(\cdot,\cdot)$ is the lower incomplete Gamma function.

4.3.2 SIC Detection Outage Probability

Unlike the ML detection method, which detects the data for all users at once, in SIC detection a user starts by cancelling the farther users' signals before detecting its own signal. Moreover, in IM-NOMA, and unlike PD-NOMA, not all users' signals are overlapping over all subcarriers, but the inter-user interference happens based on the activation done by different users. The SINR in this case can be written as follows

$$\mathrm{SINR}_n = \frac{\sum_{\ell=1}^{\mathrm{K}} \left|\sqrt{p_{(r,n)}\rho_n} h_{n\ell}\right|^2}{\sigma_n^2 + \sum_{m=1}^{n-1} P_{\text{col}}(m+1) \sum_{\ell=1}^{K} \left|\sqrt{p_{r,n}} h_{n\ell} \sum_{k=1}^{m} \sqrt{\rho_k}\right|^2}, \tag{50}$$

where the summation in the denominator is done over the nearer users' colliding signals that cannot be cancelled at user n. $P_{\text{col}}(m)$ represents the probability of collision at a specific subcarrier, i.e., the probability of the event of $m > 1$ users activate the same subcarrier, assuming the data source is uniformly random, and it is given as [12]

$$P_{\text{col}}(m) = \binom{N}{m} \left(\frac{1}{L}\right)^m \left(1 - \frac{1}{L}\right)^{N-m}. \tag{51}$$

Therefore, by substituting (50) into (46) and simplifying, the outage probability at user n can be written as follows

$$P_{o,n} = \Pr\left\{\sum_{\ell=1}^{L} |h_{n\ell}|^2 < \beta_{\text{th},n}\right\}, \tag{52}$$

where $\beta_{\text{th},n} = \frac{\sigma_n^2 \gamma_{\text{th}}}{p_{r,n}\left(\rho_n - \gamma_{\text{th}} \sum_{m=1}^{n-1} P_{\text{col}}(m+1)\left(\sum_{k=1}^{m} \sqrt{\rho_k}\right)^2\right)}$, and $\sum_{\ell=1}^{K} |h_{n\ell}|^2$ follows a Gamma distribution. Then

$$P_{o,n} = \frac{\gamma\left(K, \beta_{\text{th},n}\right)}{\Gamma(K)}, \tag{53}$$

where $\gamma(\cdot,\cdot)$ is the lower incomplete Gamma function and $\Gamma(\cdot)$ is the Gamma function.

4.3.3 SIC Detection Diversity Gain

The diversity gain is the negative slope of the outage probability curve versus the SINR at asymptotically high SINR values in a log-log scale plot, which can be written as

$$d_n = \lim_{\text{SINR}_n \to \infty} -\frac{\log\left(P_{o,n}\right)}{\log(\text{SINR}_n)}. \tag{54}$$

From (53), noting that when $\text{SINR}_n \to \infty$ the term $\beta_{\text{th},n} \to 0$, and since the expansion of $\gamma(a,x)$ near 0 is $\gamma(a,x) \approx \frac{x^a}{a}$ [43], we get

$$d_n = \lim_{\text{SINR}_n \to \infty} -\frac{\log\left(\frac{\text{SINR}_n^{-K}}{K}\right)}{\log(\text{SINR}_n)} = K. \tag{55}$$

Hence, the diversity gain in the SIC detection case equals the number of active subcarriers K by each user, which is logical since the channels over different subcarriers are assumed independent and when a user activates multiple subcarriers, its data symbols are replicated over the active subcarriers which results in the diversity gain.

4.4 Complexity Analysis

The computational complexity is usually expressed in terms of the number of real multiplications necessary for detection. In what follows, we calculate the computational complexity for both detection methods.

For the ML case all users experience the same detection complexity, as per the detection rule in (33), $6L$ real multiplications are required to perform $\sqrt{p_{r,n}}\boldsymbol{x}^{(i)} \odot \boldsymbol{h}_n$, while $2L$ multiplications are required to calculate the norm of the vector. Therefore, $8L$ multiplications are required to check a single candidate transmitted vector. Thus, since the set of all candidate transmission vectors contains a total of 2^{NB} vectors, the computational complexity at any user in IM-NOMA system applying ML detection is written as follows

$$CC_{\mathrm{ML}} = 8\mathrm{L}2^{\mathrm{NB}}. \tag{56}$$

For the SIC detection case, on the other hand, the computational complexity at a user depends mainly on the number of the performed SIC iterations which, in turn, depends on the order of the corresponding user with respect to the others. Based on (34), each iteration requires $8L2^{B}$ real multiplications. Consequently, the computational complexity in terms of the number of required real multiplications for the IM-NOMA scheme based on SIC detection technique for user n can be written as

$$CC_{\mathrm{SIC},n} = 8\mathrm{L}2^{\mathrm{B}}(N - n + 1), \tag{57}$$

where the coefficient $(N - n + 1)$ expresses the number of detection iterations performed at user n.

It is worth highlighting here that SIC provides a significant reduction in the computational complexity as compared to ML detection. Using (56) and (57), the percentage of complexity reduction due to employing SIC instead of ML at user n, denoted by CCR_n, can be expressed as follows

$$\mathrm{CCR}_n = \left(1 - 2^{B(1-N)}(N - n + 1)\right) \times 100\%, \tag{58}$$

where the maximum reduction percentage is achieved at user N, while the minimum reduction percentage occurs at the closest user (i.e., $n = 1$).

CHAPTER 5: NUMERICAL RESULTS AND DISCUSSIONS

Simulation results are presented in this section to validate the analytical formulas and to compare the proposed scheme with the classical PD-NOMA, hybrid IM-NOMA [15] and SM-NOMA [23] schemes. Users are distributed such that the distance of user n from the BS is given as $d_n = \alpha d_{n-1}$, where $d_1 = 100$m and $\alpha = 5$ is a distance multiplier. The path loss exponent is assumed as $\eta = 2.9$ and the noise power is set to $\sigma_n^2 = 10^{-10}$ Watts/Hz. The provided simulations are done for the cases of $N = 2$ and 3 users, modulation order of $M = 2$ and 4, and $K = 1$ and 2 active subcarriers per user. The total number of subcarriers is fixed equal the number of users, i.e., $N = L$ for easier comparisons with OMA schemes, and the simulations parameters are selected in all setups in which the per-user spectral efficiency is the same for all systems in comparison for the sake of fairness.

5.1 Optimal Power allocation

In order to verify our power allocation method in (29), we consider the case of two users $N = 2$, and the total transmit power at the BS is fixed at $P_t = 25$ dBm, and we plot the BER versus the power allocation coefficient of the near user ρ_1 as shown in Figure 3. The power coefficient ρ_1 is swept between 0 and 1 with a step of 0.01, while the remaining power is allocated to the far user, i.e., $\rho_2 = 1 - \rho_1$.

In Figure 3, we find that the optimal power coefficients, that yield the minimum average BER are $\rho_1 = 0.04$ and $\rho_2 = 0.96$ for the near and far users, respectively. On the other hand, using our adopted power allocation method, in (29), the corresponding power coefficients are $\rho_1 = 0.0385$ and $\rho_2 = 0.9615$, which are close to the optimal ones. In fact, our power allocation method is designed based on intuition, with the distance squared in the numerator which, partially, cancels the effect of the path loss, and thus it maximizes the received SNR at both users. In the denominator, the sum of

all squared distances is used to normalize the power coefficients. It is worth noting in this figure that allocating a very high power to the far user, i.e., $\rho_2 = 0.9$, then the near user will be able to decode and cancel the signal of the far user with low probability of error which in turn reduces the ambiguity about its own signal, hence its error performance improves significantly.

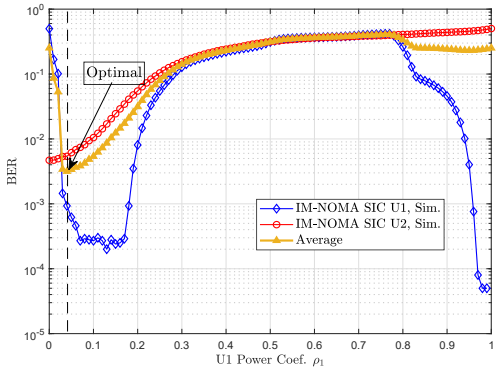

Figure 3. The BER performance of IM-NOMA versus the power coefficient of the near user with N = M = L = 2, K = 1 at atransmit power of Pt = 25 dBm.

5.2 Comparison with Classical PD-NOMA

Figure 4 shows the average BER of IM-NOMA and PD-NOMA schemes versus P_t considering $N = 2$ users, activating $K = 1$ subcarrier out of $L = 2$ available subcarriers and applying BPSK modulation, which sets the per user spectral efficiency at 2 bpcu. It is worth mentioning here that we plot the BER versus the transmit power P_t and not the SNR since the users experience different received SNR values for the same transmit power. Comparing IM-NOMA with NOMA using ML detection, a significant power gain in the favor of IM-NOMA is clearly noted, which is about 6dB at 10^{-3} BER. This is mainly due to the adoption of IM concept, as activating part of the subcarriers by each user reduces the interference between them. Furthermore, the indexing bits are transmitted with no extra power and can be detected with higher

success probability as compared to the complex modulated symbols [44], hence the adoption of IM in NOMA systems improves the error performance.

Considering the upper-bound analytical curves of IM-NOMA, the upper bound curve of the near user (U1) matches the simulation one starting at a transmit power of around 10 dBm while it needs a higher transmit power to match the far one. This is because the far user experiences a lower SNR as compared to the near one at a given transmit power.

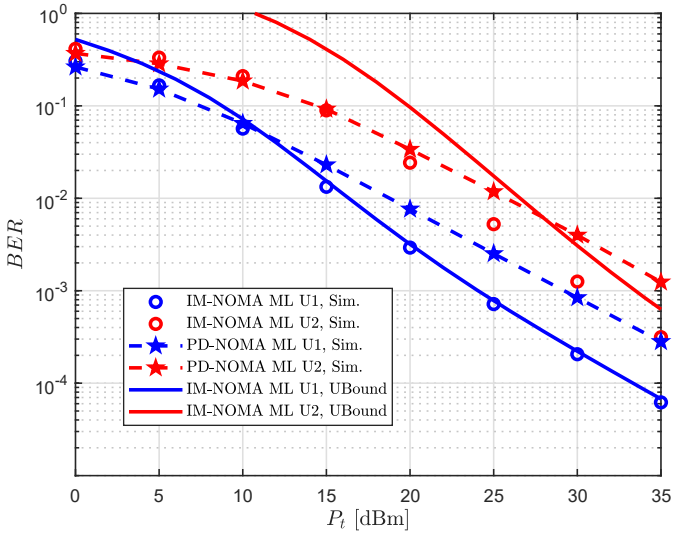

Figure 4. The average BER versus P_t at $N = L = M = 2$ for IM-NOMA ($K = 1$) and PD-NOMA schemes.

5.3 Comparison with the Literature

In Figure 5, the error performance of IM-NOMA is compared with the Hybrid IM-NOMA [15] and SM-NOMA [23], under similar configurations as in Figure 4 with two transmit antennas and one receive antenna ($N_t = 2, N_r = 1$) in SM-NOMA. Unlike the Hybrid IM-NOMA, in IM-NOMA the IM concept is applied for all users, hence the inter-user interference (or collision) probability is lower than that when we apply IM on the far user only. This explains the superiority of the near user's (U1)

performance in IM-NOMA over the Hybrid IM-NOMA especially at higher transmit power levels. However, the far user (U2) enjoys a similar performance in both schemes. Furthermore, adopting SM in multiple access schemes, as in SM-NOMA, results in involving multiple RF chains [25] which lead to poor power efficiency and higher costs. On the contrary, in IM-NOMA, the IM concept is applied on the subcarriers' indices and a higher spectral and power efficiencies can be achieved that lead to better error performance as clearly seen in the figure.

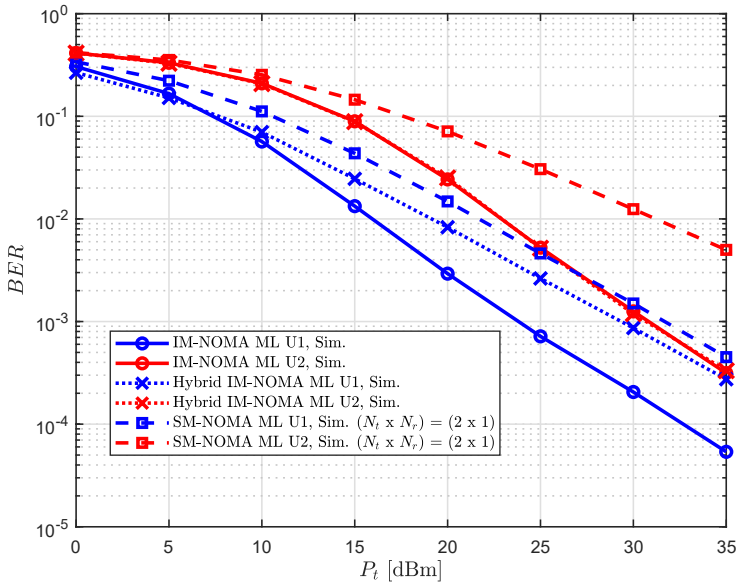

Figure 5. The average BER versus P_t at $N = L = M = 2$ for IM-NOMA ($K = 1$), hybrid IM-NOMA [15] and SM-NOMA [23] with $N_t = 2, N_r = 1$.

5.4 Multiple Active Subcarriers Per-User

Unlike the setup in Figure 4 and Figure 5 where a single subcarrier is activated per user and ML detection is applied, in Figure 6 we set $K = 2$ with $L = N = 3$, $M = 2,4$ in PD-NOMA and IM-NOMA, respectively, with SIC detection is considered in IM-NOMA. In this setup, a replicated copy of each symbol to be sent to each user is sent over two independent subcarriers which results in a higher transmit diversity gain

in IM-NOMA in comparison to that in PD-NOMA as clearly shown in Figure 6. Furthermore, the curves show that the approximated BER of the N^{th} user in IM-NOMA under SIC, using (44), matches the simulation curve starting at around $P_t =$ 40 dBm. It is worth noting here that activating multiple subcarriers per user in IM-NOMA results in coding and transmit diversity gains. The former gain is due to adopting the IM concept and reducing the inter-user interference effect, while the latter is for the reason that we replicate the transmitted symbol over multiple independent subcarriers.

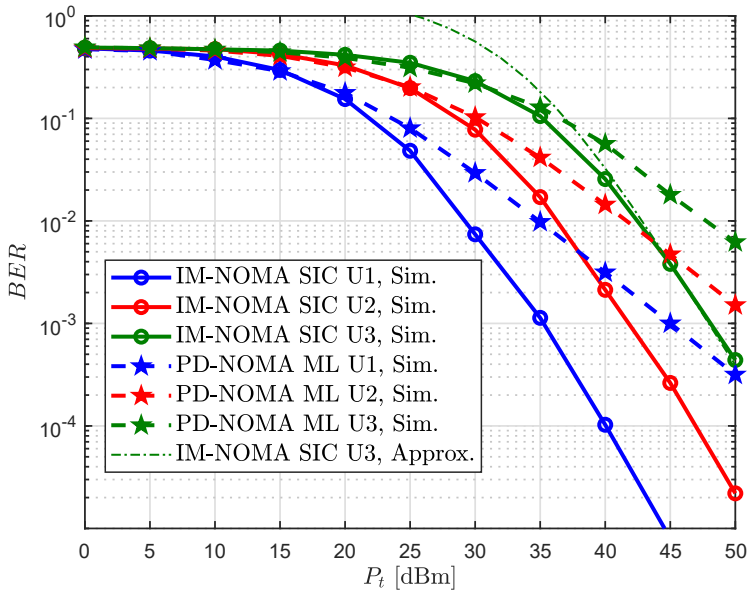

Figure 6. The average BER versus P_t at $N = L = 3$ and $M = 4,2$ for IM-NOMA $(K = 1,2)$ and PD-NOMA schemes, respectively.

5.5 Outage Probability Performance of IM-NOMA

The outage probability for both detection methods is presented in Figure 7. A setup with $N = L = M = 2$ and $K = 1,2$ is considered, while only the near user, U1, curves are shown for clarity. The perfect match between the analytical and simulation curves is clear from the figure which validates the analytical derivations of the outage

probability for both methods. As expected, the optimal ML detection method outperforms the SIC in terms of outage probability. Furthermore, the diversity gain can be clearly seen from the curves, $d_n = K$, which matches our analytical finding in (55). Similarly, the outage probability is shown in Figure 8, with $N = L = 3$ and SIC detection, which verifies the analytical derivations under different parameters and setups.

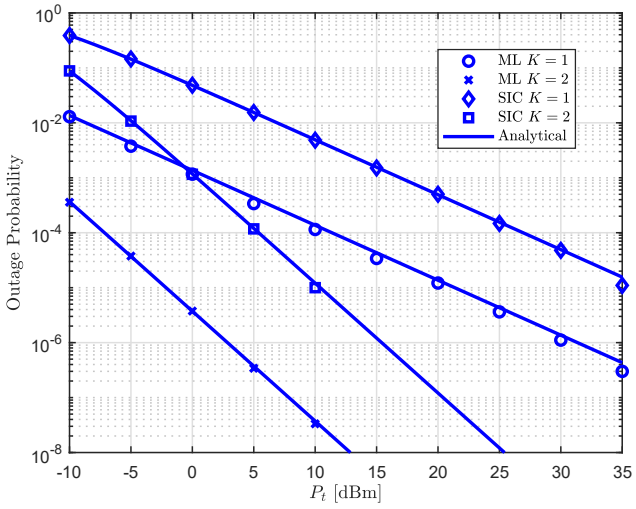

Figure 7. The outage probability of the near user, U1, versus P_t with $N = L = M = 2$, $K = 1,2$, ML and SIC detection.

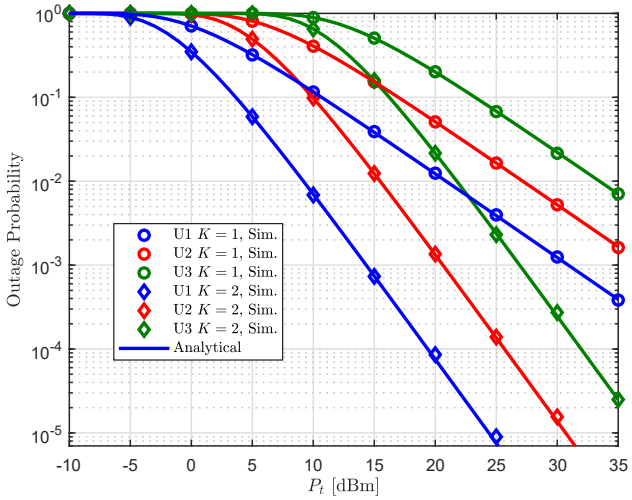

Figure 8. The outage probability versus P_t with $N = L = 3$, $M = 2$, $K = 1,2$ and SIC detection.

5.6 Computational Complexity

Finally, the average per-user computational complexity versus the total number of users N for the two schemes PD-NOMA and IM-NOMA based on both ML and SIC is plotted in Figure 9 with $L = M = 2$ and $K = 1$. As expected, the computational complexity in both schemes increases as the number of users increases. However, due to the inherited drawback of adopting the IM concept, the computational complexity induced by IM-NOMA is higher than that of PD-NOMA. On the other hand, SIC detection can significantly reduce the computational complexity induced by ML detection in both schemes at the cost of performance degradation.

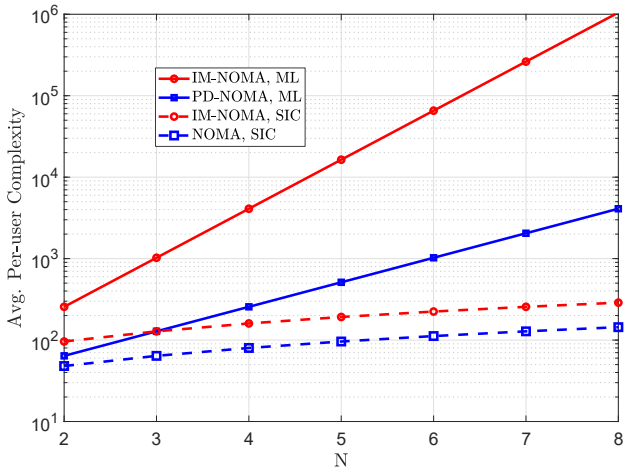

Figure 9. The average per-user computational complexity for IM-NOMA and NOMA with $M = L = 2$ and $K = 1$.

CHAPTER 6: CONCLUSIONS AND FUTURE WORK

In this thesis, both index modulation and NOMA techniques have been combined to propose a new and efficient downlink multiple access scheme, which is denoted as IM-NOMA. Several performance metrics including error and outage performance of the proposed scheme under maximum likelihood and successive interference cancellation detection techniques have been analyzed. In addition to studying the well-established NOMA scheme and deriving novel closed form expressions for its diversity gain and BER performance. Analytical findings are verified by numerical simulations where it is shown that the proposed scheme enjoys an enhanced performance over classical PD-NOMA and the related systems in the literature. Furthermore, thanks to its superior error performance, more users can be accommodated in IM-NONA as compared to classical PD-NOMA considering different configurations with an acceptable increase in the computational complexity.

Further extensions can be done by designing proper detection methods to overcome the high computational complexity of traditional methods such as ML and SIC. Additionally, the average performance of the proposed scheme needs to be assessed under more realistic users' distributions and under mobility assumptions which will involve designing more efficient power allocation and user pairing methods. Moreover, the subcarrier activation patterns can be smartly designed according to the channel quality which would further improve the proposed scheme error performance.

References

[1] H. D. Schotten, M. A. Uusitalo, J. F. Monserrat, and O. Queseth, "5G Spectrum: enabling the future mobile landscape [Guest Editorial]," *IEEE Commun. Mag.*, vol. 53, no. 7, pp. 16-17, 2015.

[2] Y. Cai, Z. Qin, F. Cui, G. Y. Li, and J. A. McCann, "Modulation and multiple access for 5G networks," *IEEE Commun. Surveys Tuts.*, vol. 20, no. 1, pp. 629-646, 2017.

[3] L. Dai, B. Wang, Y. Yuan, S. Han, I. Chih-Lin, and Z. Wang, "Non-orthogonal multiple access for 5G: solutions, challenges, opportunities, and future research trends," *IEEE Commun. Mag.*, vol. 53, no. 9, pp. 74-81, 2015.

[4] S. M. R. Islam, N. Avazov, O. A. Dobre, and K.-S. Kwak, "Power-domain non-orthogonal multiple access (NOMA) in 5G systems: Potentials and challenges," *IEEE Commun. Surveys Tuts.*, vol. 19, no. 2, pp. 721-742, 2016.

[5] H. Nikopour and H. Baligh, "Sparse code multiple access," in *2013 IEEE 24th Annual PIMRC*, pp. 332-336.

[6] S. Timotheou and I. Krikidis, "Fairness for non-orthogonal multiple access in 5G systems," *IEEE Signal Process. Lett.*, vol. 22, no. 10, pp. 1647-1651, 2015.

[7] E. Basar, M. Wen, R. Mesleh, M. Di Renzo, Y. Xiao, and H. Haas, "Index modulation techniques for next-generation wireless networks," *IEEE Access*, vol. 5, pp. 16693-16746, 2017.

[8] E. Başar, Ü. Aygölü, E. Panayırcı, and H. V. Poor, "Orthogonal frequency division multiplexing with index modulation," *IEEE Trans. Signal Process.*, vol. 61, no. 22, pp. 5536-5549, 2013.

[9] S. Althunibat and R. Mesleh, "Index modulation for cluster-based wireless sensor networks," *IEEE Trans. Veh. Technol.*, vol. 67, no. 8, pp. 6943-6950,

2018.

[10] X. Wu, H. Haas, and P. M. Grant, "Cooperative spatial modulation for cellular networks," *IEEE Trans. Commun.*, vol. 66, no. 8, pp. 3683-3693, 2018.

[11] J. Zhang, Y. Wang, J. Zhang, and L. Ding, "Polarization shift keying (PolarSK): system scheme and performance analysis," *IEEE Trans. Veh. Technol.*, vol. 66, no. 11, pp. 10139-10155, 2017.

[12] S. Althunibat, R. Mesleh, and T. F. Rahman, "A Novel Uplink Multiple Access Technique Based on Index-Modulation Concept," *IEEE Trans. Commun.*, vol. 67, no. 7, pp. 4848-4855, 2019.

[13] S. Althunibat, R. Mesleh, and K. Qaraqe, "IM-OFDMA: A Novel Spectral Efficient Uplink Multiple Access Based on Index Modulation," *IEEE Trans. Veh. Technol.*, vol. 68, no. 10, pp. 10315-10319, 2019.

[14] S. Althunibat, R. Mesleh, and K. Qaraqe, "Quadrature Index Modulation Based Multiple Access Scheme for 5G and Beyond," *IEEE Commun. Lett.*, vol. 23, no. 12, pp. 2257-2261, 2019.

[15] A. Tusha, S. Dogan, and H. Arslan, "A Hybrid Downlink NOMA with OFDM and OFDM-IM for Beyond 5G Wireless Networks," *IEEE Signal Process. Lett.*, 2020.

[16] S. Doğan, A. Tusha, and H. Arslan, "NOMA With Index Modulation for Uplink URLLC Through Grant-Free Access," *IEEE Journal of Selected Topics in Signal Processing*, vol. 13, no. 6, pp. 1249-1257, 2019.

[17] J. Li, Q. Li, S. Dang, M. Wen, X.-Q. Jiang, and Y. Peng, "Low-Complexity Detection for Index Modulation Multiple Access," *IEEE Trans. Wireless Commun.*, 2020.

[18] A. Almohamad, M. Hasna, S. Althunibat, S. Özyurt, and K. Qaraqe, "Low

Complexity Constellation Rotation-based SIC Detection for IM-NOMA Schemes," in *2020 IEEE 92nd Vehicular Technology Conference (VTC2020-Fall)*, 2020, pp. 1-5.

[19] T. Wang, F. Yang, and J. Song, "Novel Index Modulation Aided Non-Orthogonal Multiple Access for Visible Light Communication," in *2019 IEEE GLOBECOM Conference*, pp. 1-6.

[20] M. B. Shahab, S. J. Johnson, M. Shirvanimoghaddam, M. Chafii, E. Basar, and M. Dohler, "Index Modulation Aided Uplink NOMA for Massive Machine Type Communications," *IEEE Wireless Communications Letters*, pp. 1-1, 2020.

[21] X. Chen, M. Wen, and S. Dang, "On the Performance of Cooperative OFDM-NOMA System With Index Modulation," *IEEE Wireless Communications Letters*, vol. 9, no. 9, pp. 1346-1350, 2020.

[22] R. Y. Mesleh, H. Haas, S. Sinanovic, C. W. Ahn, and S. Yun, "Spatial modulation," *IEEE Transactions on vehicular technology*, vol. 57, no. 4, pp. 2228-2241, 2008.

[23] Z. Wang, J. Cao, and others, "NOMA-based spatial modulation," *IEEE access*, vol. 5, pp. 3790-3800, 2017.

[24] Q. Li, M. Wen, E. Basar, H. V. Poor, and F. Chen, "Spatial modulation-aided cooperative NOMA: Performance analysis and comparative study," *IEEE Journal of Selected Topics in Signal Processing*, vol. 13, no. 3, pp. 715-728, 2019.

[25] Y. Sun, J. Wang, L. Shi, X. Zhang, and J. Song, "On RF-Chain Limited Spatial Modulation Aided NOMA: Spectral Efficiency Analysis," in *2019 IEEE Globecom Workshops (GC Wkshps)*, pp. 1-5black.

[26] Y. Chen, L. Wang, Y. Ai, B. Jiao, and L. Hanzo, "Performance analysis of NOMA-SM in vehicle-to-vehicle massive MIMO channels," *IEEE Journal on Selected Areas in Communications,* vol. 35, no. 12, pp. 2653-2666, 2017.

[27] C. Zhong, X. Hu, X. Chen, D. W. K. Ng, and Z. Zhang, "Spatial modulation assisted multi-antenna non-orthogonal multiple access," *IEEE Wireless Communications,* vol. 25, no. 2, pp. 61-67, 2018.

[28] E. Arslan, A. T. Dogukan, and E. Basar, "Index Modulation-Based Flexible Non-Orthogonal Multiple Access," *IEEE Wireless Communications Letters,* vol. 9, no. 11, pp. 1942-1946, 2020.

[29] A. Almohamad, S. Althunibat, M. Hasna, and K. Qaraqe, "On the Error Performance of Non-orthogonal Multiple Access Systems," in *2020 International Conference on Information and Communication Technology Convergence (ICTC)*, 2020, pp. 116-121.

[30] Z. Yang, Z. Ding, P. Fan, and G. K. Karagiannidis, "On the performance of non-orthogonal multiple access systems with partial channel information," *IEEE Trans. Commun.,* vol. 64, no. 2, pp. 654-667, 2015.

[31] M. Alouini and A. J. Goldsmith, "A unified approach for calculating error rates of linearly modulated signals over generalized fading channels," *IEEE Transactions on Communications,* vol. 47, no. 9, pp. 1324-1334, 1999.

[32] J. W. Craig, "A new, simple and exact result for calculating the probability of error for two-dimensional signal constellations," in *MILCOM 91 - Conference record*, 1991, pp. 571-575 vol.2.

[33] A. Jeffrey and D. Zwillinger, *Table of integrals, series, and products*. Elsevier, 2007.

[34] L. Bariah, S. Muhaidat, and A. Al-Dweik, "Error Probability Analysis of Non-

Orthogonal Multiple Access Over Nakagami- m Fading Channels," *IEEE Transactions on Communications,* vol. 67, no. 2, pp. 1586-1599, 2019.

[35] A. Almohamad, M. O. Hasna, S. Althunibat, and K. Qaraqe, "A Novel Downlink IM-NOMA Scheme," *IEEE Open Journal of the Communications Society,* vol. 2, pp. 235-244, 2021.

[36] A. Almohamad, S. Althunibat, M. Hasna, and K. Qaraqe, "A Downlink Index-Modulation Based Nonorthogonal Multiple Access Scheme," in *2020 IEEE 31st Annual International Symposium on Personal, Indoor and Mobile Radio Communications*, 2020, pp. 1-6.

[37] S. Mounchili and S. Hamouda, "Pairing Distance Resolution and Power Control for Massive Connectivity Improvement in NOMA Systems," *IEEE Trans. Veh. Technol.,* vol. 69, no. 4, pp. 4093-4103, 2020.

[38] A. Benjebbovu, A. Li, Y. Saito, Y. Kishiyama, A. Harada, and T. Nakamura, "System-level performance of downlink NOMA for future LTE enhancements," in *2013 IEEE Globecom Workshops*, pp. 66-70.

[39] F. redFang, H. Zhang, J. Cheng, and V. C. M. Leung, "Energy-efficient resource allocation for downlink non-orthogonal multiple access network," *IEEE Transactions on Communications,* vol. 64, no. 9, pp. 3722-3732, 2016.

[40] M. K. Simon, S. M. Hinedi, and W. C. Lindsey, *Digital communication techniques: signal design and detection*. Prentice Hall PTR, 1995.

[41] H. Jasiulewicz and W. Kordecki, "Convolutions of Erlang and of Pascal distributions with applications to reliability," *Demonstratio Mathematica,* vol. 36, no. 1, pp. 231-238, 2003.

[42] A. Almohamad, S. Althunibat, M. Hasna, and K. Qaraqe, "A Downlink Index-Modulation Based Nonorthogonal Multiple Access Scheme," in *2020 IEEE*

31st Annual International Symposium on Personal, Indoor and Mobile Radio Communications, pp. 1-6.

[43] I. Thompson, "A note on the real zeros of the incomplete gamma function," *Integral Transforms and Special Functions*, vol. 23, no. 6, pp. 445-453, 2012.

[44] M. Wen, B. Ye, E. Basar, Q. Li, and F. Ji, "Enhanced orthogonal frequency division multiplexing with index modulation," *IEEE Transactions on Wireless Communications*, vol. 16, no. 7, pp. 4786-4801, 2017.